Advances in Geo-Energy Research

Vol. 3, No. 2, p. 165-174, 2019
www.astp-agr.com

Original article

Experimental and numerical simulation of water adsorption and diffusion in shale gas reservoir rocks

Weijun Shen[1]*, Xizhe Li[2], Abdullah Cihan[3], Xiaobing Lu[1], Xiaohua Liu[2]

[1]*Institute of Mechanics, Chinese Academy of Sciences, Beijing 100190, P. R. China*

[2]*PetroChina Research Institute of Petroleum Exploration and Development, Beijing 100083, P. R. China*

[3]*Energy Geosciences Division, Lawrence Berkeley National Laboratory, Berkeley, CA 94720, USA*

(Received Feburary 14, 2019; revised Feburary 27, 2019; accepted March 4, 2019; available online March 8, 2019)

Citation:
Shen, W., Li, X., Cihan, A., Lu, X., Liu, X. Experimental and numerical simulation of water adsorption and diffusion in shale gas reservoir rocks. *Advances in Geo-Energy Research*, 2019, 3(2): 165-174, doi: 10.26804/ager.2019.02.06.

Corresponding author:
*E-mail: wjshen763@imech.ac.cn

Keywords:
Shale gas
water adsorption and diffusion
capillary condensation
water retention
GAB model

Abstract:
Despite the success of deep horizontal drilling and hydraulic fracturing in yielding large production increases from unconventional shale gas reservoirs, uncertainties associated with basic transport processes require understanding in order to improve efficiency and minimize environmental impacts. The hydraulic fracturing process introduces large volumes of water into shale gas reservoirs, most of which remains unrecoverable and interferes with gas production. In this study, the water adsorption and diffusion measurements of the Longmaxi Formation shale were conducted at 30 °C and 50 °C for relative humidities from 11.1% to 97.0%. Based on the experiment, a computational model based on the Maxwell-Stefan diffusion equation was constructed to analyze water adsorption and diffusion in shale rocks, and the Guggenheim-Anderson-de Boer (GAB) isotherm for gas adsorption was included in the model. The results show that water adsorption isotherms of shales belong to type II curve, including the monolayer, multilayer adsorption and capillary condensation, and the GAB model can be used to describe the water adsorption process in shale rocks. With the increasing of relative pressure, the water adsorption of shale increases, and the organic carbon content and temperature strengthen the water adsorption in shale. The capillary pressure can reach the order of several hundreds of MPa after the hydraulic fracturing process, and it results in a large amount of fracturing fluid retained in shale gas reservoirs. Furthermore, the simulation of water adsorption and diffusion in shale rocks is less than the experimental value, which further indicates that capillary condensation occurs in shale rocks.

1. Introduction

With the increasing demand for the world economy, the development of unconventional shale gas resource has attracted extensive attention worldwide, which has gradually become the strategic supplemental of conventional oil and gas resources (Shen et al., 2017; Tokunaga et al., 2017). Shale gas is a kind of unconventional natural gas that is adsorbed, free or dissolved within the pores of shale rocks (Wei et al., 2013; Shen et al., 2018). Compared with conventional gas reservoirs, shale gas reservoirs are characterized by low porosity and ultra-low permeability, so horizontal drilling and hydraulic fracturing are the key technologies to produce gas from shale gas reservoirs (Cheng, 2012; Xu et al., 2015; Shen et al., 2016; Wei et al., 2016). In the last few years, due to the advances in horizontal drilling and hydraulic fracturing technologies, gas production from shale formations has drastically increased in the United States (Li et al., 2015; Tokunaga et al., 2017). According to the statistics from the U.S. Energy Information Administration, about 16.86 trillion cubic feet of dry natural gas was produced from shale resources in the United States, and the proportion was about 62% of total U.S. dry natural gas production in 2017 (International Energy Agency, 2018). The large-scale development of shale gas influenced the world natural gas market and energy structure, and thus many major resource countries in the world have increased the exploration and development of shale gas reservoirs.

During the hydraulic fracturing process, a large amount of water-based fracturing fluid was injected into the shale formation while only a small amount of injected fluid returned to the ground, and most of the fluid remained in the shale formation to interfere with the development of shale gas reservoirs (King, 2010; Cheng, 2012). The mineral composition of shale is complex and contains a variety of clay

https://doi.org/10.26804/ager.2019.02.06.

minerals such as montmorillonite, kaolinite and illite (Shen et al., 2017). There exist charges on the surface of clay minerals, and water molecules and clay particles can be formed by hydrogen bonding, electrostatic force and intermolecular force, which forms a certain thickness of water film (Li et al., 2017). Chenevert (1970, 1998) and Ai-Awad and Smart (1996) believed that the main cause of shale failure was the hydration of shale in contact with water, and the migration of water and ions changed the physical and chemical state of shale, which resulted in the wellbore instability. Wu et al. (2014) considered that the flow capacity of gas phase when the saturation of pore water was 20% was lower than that on the drying condition by the gas-water-flow experiment in 1D nanoscale channels. Chang et al. (2013), Li et al. (2017) and Qi et al. (2018) believed that the existence of adsorbed water had a great influence on the adsorption ability of shale, and it would occupy the surface of inorganic hydrophilic mineral, which caused the decrease of shale adsorption ability. The water adsorption in shale not only influences the physical, chemical and mechanical properties of shale, but also affects the adsorption, diffusion and flow capacity of shale gas. Consequently, there is greatly significant to understand the water adsorption and diffusion in shale rocks so as to optimize extraction conditions.

In the past few years, many laboratory experiments have been carried out by the domestic and foreign scholars to understand the changing process of shale in contact with water. Odusina (2011), and Dehghanpour et al. (2013) observed that shale could absorb more water, which was attributed to the absorption of water molecules in clay. Gao et al. (2013) pointed out that the expansion ratio of shale in fracturing fluid was lower than that in formation water and distilled water using comparison experiments. Makhanov et al. (2014) and Ge et al. (2015) conducted water absorption experiments of shale in different regions and found that the imbibition volume was much larger than the initial pore volume, which was mainly due to the absorption water molecules of clay. Shen et al. (2017) believed that fracturing fluids were imbibed into the formation matrix and complicated physical and chemical effects happen between fluids and shale, and liquid diffusion into deeper matrix and micro-fracture induced by water-rock reaction were treated as the main mechanisms of water block. Although there are a few studies on the water adsorption of shale, a detailed understanding of water adsorption and diffusion in shale gas reservoir rocks is lacking. Therefore, there is a necessity to understand the behavior of water adsorption and diffusion in shale so as to optimize fracturing treatment and enhance gas productivity in shale gas reservoirs.

In this study, the measurements of water adsorption and diffusion in the Longmaxi Formation shale were conducted using the gravimetric techniques at 30 °C and 50 °C for relative humidities up to 97%. The water adsorption type of shale rocks was determined and the related effects of TOC and temperature were analyzed. The Guggenheim-Anderson-de Boer (GAB) and Frenkel-Halsey-Hill (FHH) models were used to fit the water adsorption isotherm in shale, and the relationships among water adsorption, saturation and water retention in shale pores were determined to illustrate the water adsorption and diffusion process. In order to better understand the process, a computational model based on the Maxwell-Stefan diffusion equation was constructed to analyze water adsorption and gas diffusion in shales, and the GAB isotherm for gas adsorption was included in the model.

2. Theory

The hydration of clay minerals is one of the important interaction processes between the rock matrix and pore fluid. The adsorption isotherm model is a useful approach to describe the hydration process of clay minerals (Chenevert, 1970). There are a number of adsorption isotherm models developed over the years to describe the adsorption process, such as the Langmuir, Freundlich, Brunauer-Emmett-Teller (BET), GAB, and FHH models (Foo and Hameed, 2010). According to the porous structure and the extended multilayer sorption phenomena, Tien (1994) presented five general type curves of adsorption isotherms that identify the adsorption mechanism. Tandanand (1985) and Shen et al. (2018) considered that the water adsorption isotherm of shale rocks was comparable to the isotherm of type II or III, and the most common adsorption isotherm models that expressed the multilayer adsorption phenomena were GAB model and FHH model.

2.1 GAB model

The GAB isothermal adsorption model developed by Guggenheim (1996), Anderson (1946) and Boer (1953), is a modification of the Langmuir and BET theories of adsorption isotherms. It assumes that the state of adsorbate molecules in the second layer is similar to those in superior layers, but different from those in the liquid state. The isotherm model has a third constant, k, which is related to the difference between the heat of sorption and the heat of condensation (Anderson, 1946). The GAB model can be written as follows:

$$q = \frac{q_m k a_w c}{(1 - k a_w)(1 - k a_w + c k a_w)} \tag{1}$$

where q is the amount of gas adsorption; q_m is the maximum amount of adsorption for the monolayer; a_w is the water activity, $a_w = p/p_0$; c and k are the GAB constants, respectively. It is noted that when k is equal to 1, the GAB model becomes the BET model.

2.2 FHH model

Based on the multi-layer adsorption with capillary condensation, Frenkel (1946), Halsey (1948) and Hill (1949) proposed the FHH isotherm model of fractal interface to describe the adsorption process. The model assumes the adsorbate as a uniform thin layer of liquid on the homogeneous solid surface, and the molecule in the adsorbed layer will feel different potentials. And the FHH model can be expressed as follows:

$$\left(\frac{q}{q_m}\right)^n = \frac{A}{-\ln\left(\frac{p}{p_0}\right)} \tag{2}$$

Table 1. Some measured properties of shale rocks used in this study.

Shale sample	Depth (m)	OCC (%)	Surface area (m^2/g)	Mineral composition
Shale A	1987.85	1.60	16.16	Plagioclase, pyrite
Shale B	1982.73	2.30	16.06	Plagioclase, pyrite
Shale C	1966.31	4.50	23.72	Plagioclase, pyrite
Shale D	1986.13	6.30	29.38	Plagioclase, pyrite, calcite

$$A = \frac{\varepsilon_0}{RTx_m^n} \tag{3}$$

where n is the FHH isothermal constant, which is related to the adsorbate, adsorbent and temperature; ε_0 is the adsorption potential of the solid surface; x_m^n is the monolayer adsorption thickness; T is the temperature; R is the gas constant; and the remaining parameters are the same as above.

2.3 Water adsorption and saturation

The water content of the rock is the ratio of the volume of water contained in rock pores to the volume of dry rock, which can be expressed as the volumetric water content (Genuchten, 1980). According to the result from Shang et al. (1995), the amount of adsorption at any given temperature and pressure can be converted to saturation, which can be described as follows:

$$S_w = \frac{(1-\varphi)}{\varphi}\frac{\rho_r}{\rho_w}q \tag{4}$$

where S_w is the volumetric water saturation of the rock; φ is the porosity of the rock; ρ_r and ρ_w are the densities of the rock and the adsorbed phase, respectively; and the remaining parameters are the same as above.

2.4 Saturation and capillary pressure

While the adsorption process can be described by appropriate isotherm models, the condensation phenomena is well represented by the Kelvin equation (Adamson and Gast, 1967), which can be described as follows:

$$RT\ln\left(\frac{p}{p_0}\right) = \frac{2\gamma V_m}{r} \tag{5}$$

where R is the universal gas constant; T is the temperature; γ is the interfacial tension; V_m is the molar volume of a condensed droplet; r is the radius of the droplet; and the remaining parameters are the same as above.

In conjunction with Laplace's equation (Adamson and Gast, 1967), the capillary pressure can be expressed as follows:

$$\Delta P = -\frac{RT}{V_m}\ln\left(\frac{p}{p_0}\right) \tag{6}$$

where ΔP is the capillary pressure.

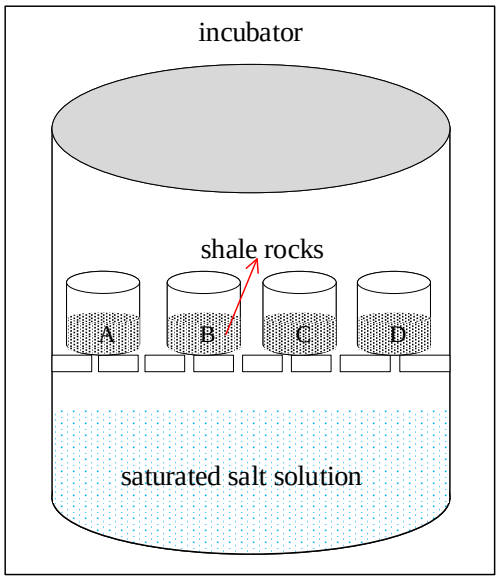

Fig. 1. Schematic apparatus of water adsorption and diffusion in shale rocks.

3. Experimental materials and methods

3.1 Experimental materials

In this study, the shale rocks were obtained from various depths within the Longmaxi Formation in southern China, which ranges from 1966.31 m to 1987.85 m. These shale samples were crushed indoors and were separated based on different particle sizes using screens of different mesh sizes (250 $\sim$ 800 μm). And then the organic carbon content (OCC), specific surface area and mineral composition were measured with the TOC analyzer, Autosorb-1 surface-specific analyzer and X-ray diffraction, respectively. The measured properties of these shale rocks are illustrated in Table 1.

3.2 Experimental methods

The water adsorption and diffusion measurements in shale were performed by means of the gravimetric techniques at 30 °C and 50 °C, and the schematic apparatus of the measurement was illustrated in Fig. 1. In the study, the shale rocks (Shale A, Shale B, Shale C and Shale D) with the particle range of 500 - 800 μm were selected and confined within an incubator, which was a controlled humidity environment. The environment was created by the saturated salt solutions illustrated in

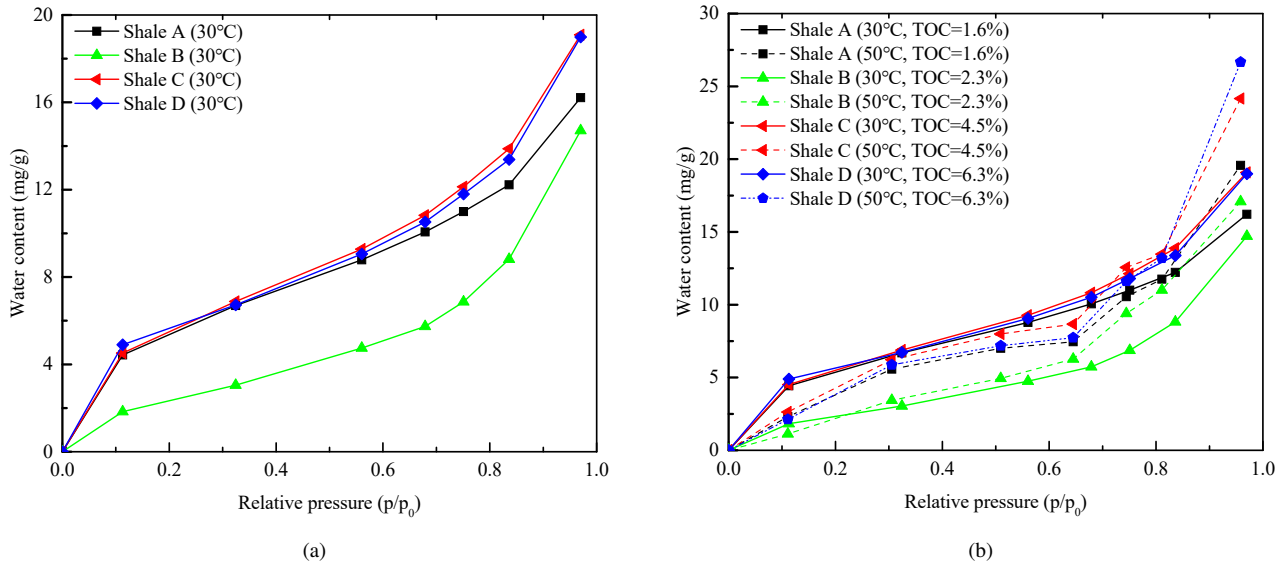

Fig. 2. Measured water adsorption isotherms of shale rocks.

Table 2 (Greenspan, 1977), and the solutions controlled the relative humidity (RH) ranging from 11.1% to 97.0%. The relative humidity, also known as relative pressure (p/p_0), is the ratio of water vapor pressure in the air (p) relative to the saturated water vapor pressure (p_0) (Shen et al., 2018). After oven-drying (120 °C), the adsorption isotherm and diffusion measurement of shale rocks was conducted at 30 °C with a saturated LiCl salt solution, and then were weighted daily after cooling to room temperature until the equilibrium. The change in shale mass during the process was taken as the amount of adsorbed water. After the completion for LiCl salt solution, the subsequent experiments with $MgCl_2$, NaBr, KI, NaCl, KCl and K_2SO_4 salt solutions were conducted at 30 °C, and the measurements at 50 °C the same as that at 30 °C.

4. Results and discussion

4.1 Water adsorption isotherm

The curves of water adsorption isotherm for different shale rocks are illustrated in Fig. 2. As can be seen from the Fig. 2(a), the water adsorption isotherm curves in shale show a similar feature. At the relative pressure below 0.65, the amount of adsorbed water seems be approximated by a linear function of relative pressure, and the monolayer-multilayer adsorption occurs in shale. However, the linear relationship is broken down as the relative pressure increases and the adsorbed water increases rapidly with relative pressure. The change in the shape of water adsorption isotherm indicates that capillary condensation takes place, and its contribution to total adsorbed water onto the shale rocks becomes more significant as relative pressure increased further. According to the classification of the International Union of Pure and Applied Chemistry (IUPAC), the isotherm types of these shale rocks belong to type II, which is common in the microporous porous media (Sing, 1985). From the result of the Fig. 2(b), we can see that the effect of temperature on water adsorption isotherm also seems to be similar. Generally, the effect is small at the low relative pressure, and then becomes more appreciable at the high relative pressure. One possible cause for the phenomenon is chemical interaction of water with the rock surface. Secondly, the presence of minerals will cause the situation, and there are minerals present in the shale rocks that will dissolve in the adsorbed water and have their appropriate effects on the phenomenon, which may in turn affect the amount of water adsorbed at different temperatures, especially at the high relative pressure. In addition, it is also related to OCC, and organic matter in shale rocks contains many micro- and nanopores, which will influence the adsorption process (Tokunaga et al., 2017). It can be seen that the adsorption capacity of the higher OCC is more than that of lower OCC, which is an indication that the OCC is beneficial to water adsorption of shale rocks.

Table 2. Saturated salt solutions used to control relative humidity.

Salt solution	Relative humidity (%)	
	30 °C	50 °C
LiCl	11.28	11.10
$MgCl_2$	32.44	30.54
NaBr	56.03	50.93
KI	67.89	64.49
NaCl	75.09	74.43
KCl	83.62	81.10
K_2SO_4	97.00	95.82

4.2 Adsorption isotherm fitting

According to the experimental adsorption measurements of shale rocks at 30 °C and 50 °C, the adsorption models of GAB

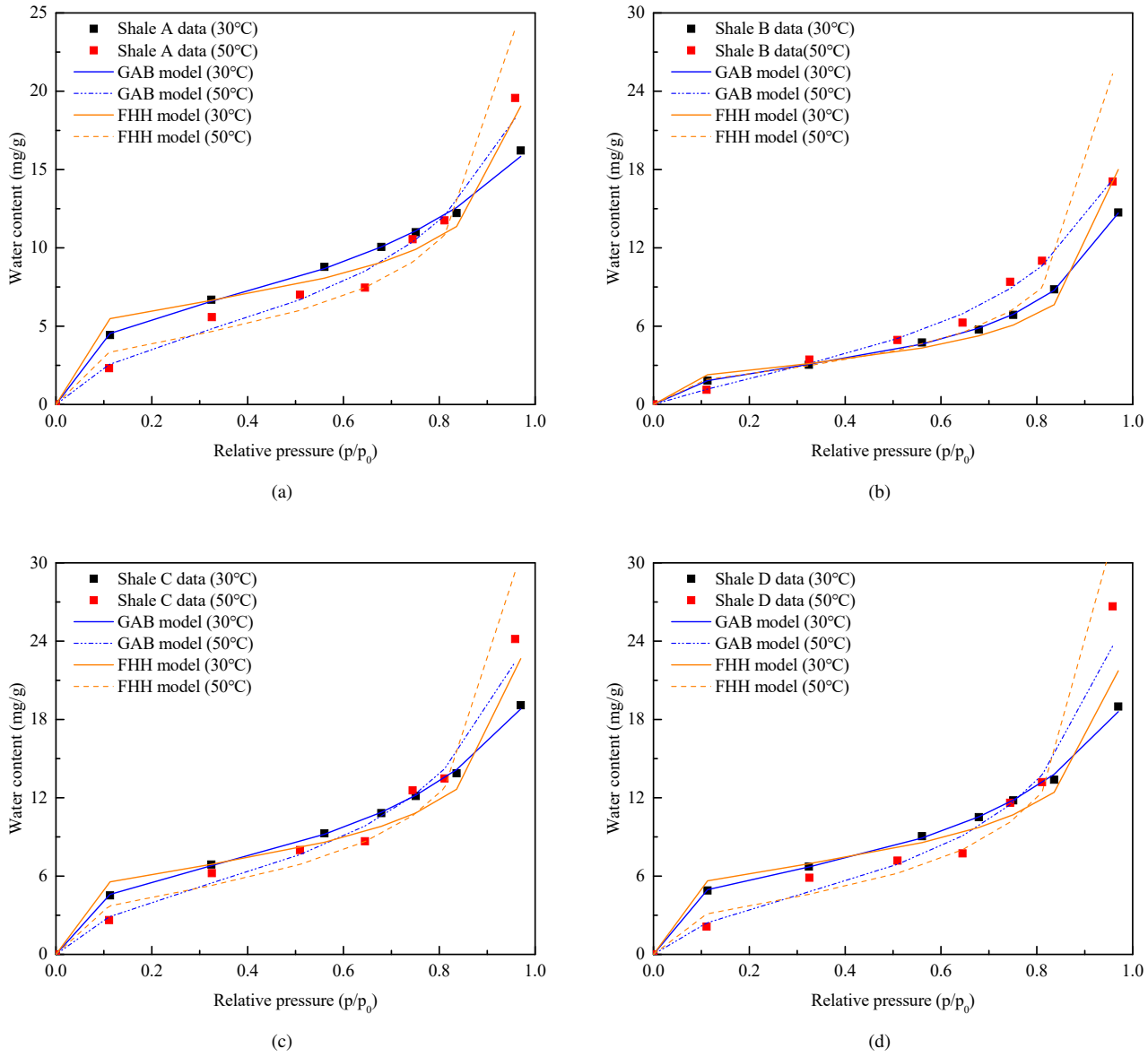

Fig. 3. Comparisons of isothermal adsorption models fitted experimental data in shale rocks.

and FHH were applied to fit the experimental data, as shown in Fig. 3. From the result of Fig. 3, although there is certain deviation when the relative pressure is greater than 0.93, the fitting of GAB model agrees well with the experimental data in general. Compared with the GAB model, the FHH model deviates greatly from the fitting results of the experiment, particularly at high relative pressure. The FHH isotherm model is widely used to describe the phenomenon of capillary condensation in porous materials at high relative pressure (Hill, 1949). During the adsorption process, the amount of water adsorbed in shale increases greatly with high relative pressure, which indicates that the capillary condensation takes place in shale pores. Consequently, it can be seen that the equilibrium of water adsorption and diffusion in shale rocks is a complicated process including single-layer, multi-layer adsorption and capillary condensation.

4.3 Water saturation and capillary pressure

According to the Eq. (5) - Eq. (7), the relationship between the amount of water adsorbed and relative pressure in shales can be converted into the relationship between capillary pressure and water saturation, as illustrated in Fig. 4. In the study, the water saturation is calculated from the amount of water adsorbed using the bulk water density of 0.996 g/cm^3 (30 °C) and 0.988 g/cm^3 (50 °C), respectively. As can be seen from Fig. 4(a), the water saturation is very low at relative pressure below 0.65, and the water saturation of shale increases rapidly with the higher relative pressure. The reason is that the large amount of water adsorbed in the capillary pores will condense into liquid droplets. From the result of Fig. 4(b), we can see that capillary pressure is considerably large, which can reach hundreds of MPa in the low saturation. Thus, it is far from

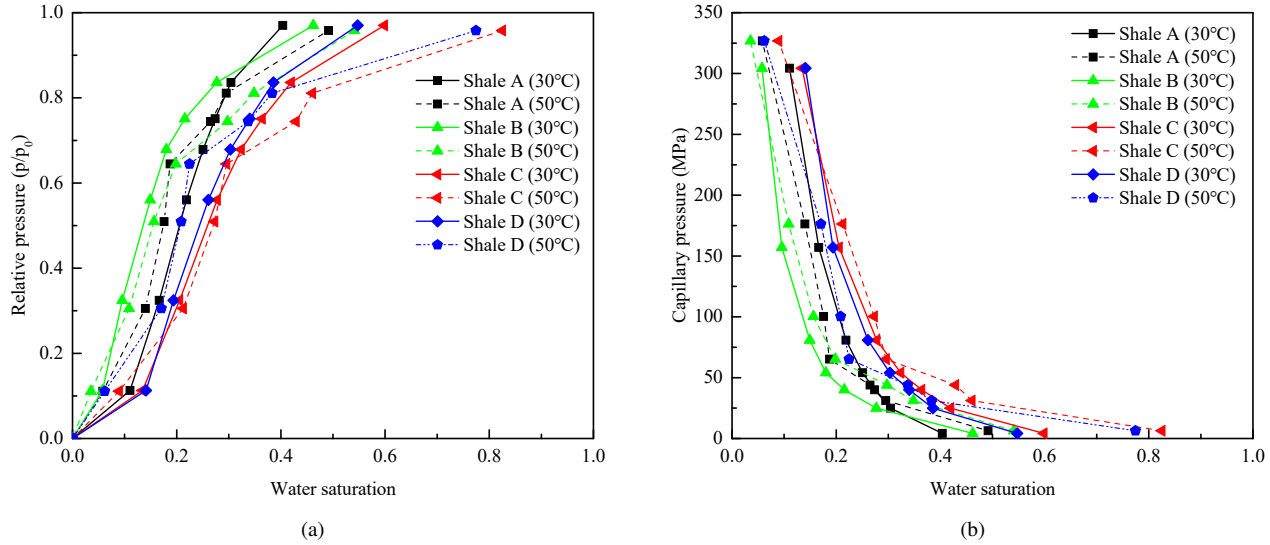

Fig. 4. Water saturation versus capillary pressure for different shale rocks.

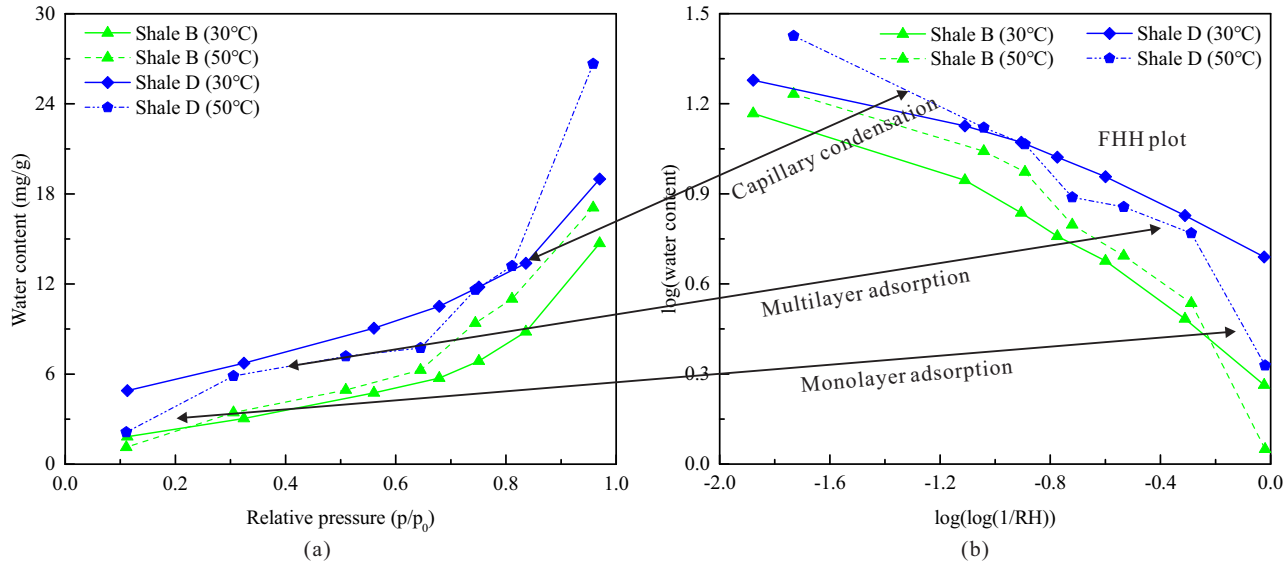

Fig. 5. Relationship between relative pressure and mechanism for water retention in shale rocks.

easy for water retention to return to the ground, which results in considerable water retention in shale reservoirs.

4.4 Water retention in shale pores

The FHH model considers the adsorbate as a uniform thin layer of liquid on the homogeneous solid surface, which is commonly used to analyze and describe the adsorption process on the surface of the flat solid (Prost et al., 1998). In the study, the FHH plot can be achieved by plotting log(water content (mg/g)) as a function of log(1/(RH)), which is illustrated in Fig. 5. From the result of Fig. 5, it can be perceived that the FHH plot provides a useful plot for dividing three portions of adsorbed water in shale rocks, which includes monolayer adsorption, multilayer adsorption and capillary condensation. At the low relative pressure, the monolayer adsorption occurs in shale rocks, and the water is adsorbed on the hydrophilic sites in shale. As relative pressures increase, the multilayer adsorption will take place in free surfaces. At the higher relative pressure, the capillary condensation arises in shale pores, which leads to the amount of adsorbed water significantly increase.

5. Mathematical model and model description

5.1 Mathematical model

In order to better understand the process of water adsorption and diffusion in shale rocks, a computational model based on the Maxwell-Stefan diffusion equation was constructed to analyze water adsorption and gas diffusion in shale rocks. Based on the above experiment results, the GAB isotherm

Table 3. Some properties of the shale model for water adsorption and diffusion.

Property	Value	Unit
Model radius	5.0×10^{-4}	m
Porosity (Por)	5	%
Diffusivity (D_{12})	2.8×10^{-5}	m^2
Effective diffusivity (D_{e12})	$(D_{12}) \times Por^{1.5}$	m^2
GAB coefficient (C_o)	9.81	1
GAB coefficient (k)	0.76	1
The maximum adsorption amount for the monolayer of GAB (V_{max})	4.22×10^{-3}	kg/kg
Air molar mass (M_{air})	2.8×10^{-2}	kg/mol
Water molar mass (M_{h_2o})	1.8×10^{-2}	kg/mol
Water density (ρ_{h_2o})	9.96×10^2	kg/m^3
Rock density (ρ_{grain})	2.7×10^3	kg/m^3
Standard atmosphere (P)	1.01×10^5	Pa
Temperature (T)	30 (50)	°C
Saturated vapor pressure (P_{swat})	$610.78e^{(T/(T+238.3)\times 17.27)}$	Pa
Saturated mole fraction	$RH \times (P_{swat}/P)$	1
Saturated mass fraction	$X_{sat}/M_{h_2o}/\left(X_{sat} \times M_{h_2o} + (1 - X_{sat}) \times M_{air}\right)$	1

for gas adsorption was included in the model. For the multi-component gas, the Maxwell-Stefan equation can describe the process of gas diffusion (COMSOL, 2015), which is expressed as follows:

$$\delta_{ts}\rho\frac{\partial w_i}{\partial t} + \nabla \cdot j_i + \rho u \cdot \nabla w_i = R_i \tag{7}$$

$$j_i = -\left(\rho w_i \sum\nolimits_K D_{ik} d_k + D_i^T \frac{\nabla T}{T}\right) \tag{8}$$

$$d_k = \nabla X_K + (X_K - W_K)\frac{\nabla P}{P} \tag{9}$$

$$X_K = \frac{W_K}{M_K} M_n \tag{10}$$

$$M_n = \left(\sum_i \frac{W_k}{M_k}\right)^{-1} \tag{11}$$

$$\delta_{ts}\rho\frac{\partial wh2o}{\partial t} + \nabla \cdot (-\rho wh2o \sum\nolimits_K D_{1k}(\nabla X_K + (X_K - W_K)\frac{\nabla p}{p}) - D^T\frac{\nabla T}{T}) = R - \rho u \cdot \nabla wh2o \tag{12}$$

where δ_{ts} is the time-scale coefficient; ρ is the density; D_{1k} is the diffusion coefficient of Maxwell-Stefan; P is the pressure; T is the temperature; u is the velocity; D_i^T is the multi-component thermal diffusivity; M is the molecular weight; R is the reaction rate.

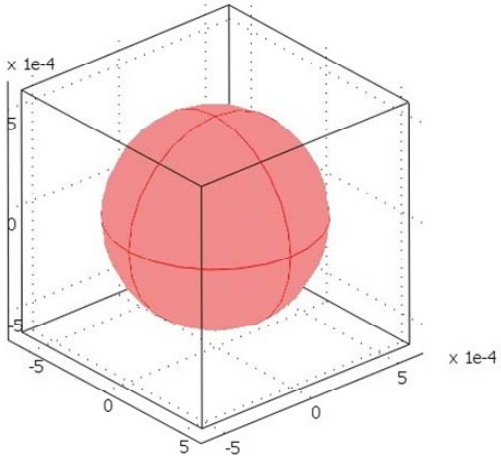

Fig. 6. Sphere domain used for modeling water diffusion and adsorption in shale rocks.

5.2 Model description

In order to better understand the process of water adsorption and diffusion in shale rocks, a three-dimensional model of microscale shale particle was established. The geometry of the shale particle was illustrated in Fig. 6 and the properties of the model were summarized in Table 3. In the study, the shale model assumptions are as follows: (1) The internal water vapor concentration of shale particles is zero at the initial time; (2) The outer boundary is under saturated water vapor pressure controlled by saturated salt solution with different humidity. And all external surfaces are kept at saturation vapor pressure. Here the shale B was selected to simulate water adsorption

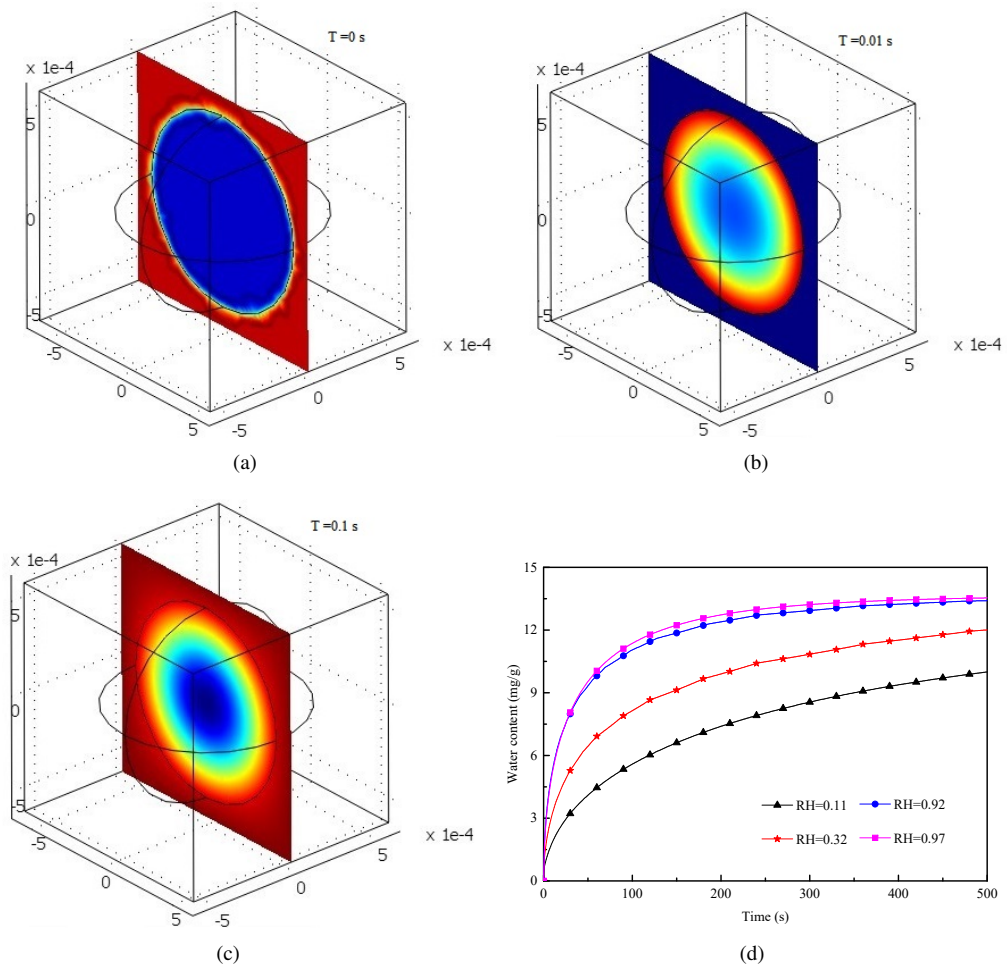

Fig. 7. Adsorbed H_2O concentration along a slice passing through center of the sphere from T = 0 to T = 0.1 s, and water content versus time with different relative humidities (Shale B).

and diffusion in shale rocks, and the simulation was run in the platform of COMSOL Multiphysics Software (COMSOL, 2015).

5.3 Simulation results

At the initial stage, the shale particles are dry, which means that the internal water concentration of the shale particle is zero. When the relative humidity in the shale particle is less than that in the external environment, the shale particle will absorb water vapor. That is, the water will enter the shale particle by the diffusion until that the relative humidity of the shale particle is equal to the outside humidity, and it will reach the state of adsorption dynamic equilibrium. The adsorbed H_2O concentration along a slice passing through center of the sphere and water content versus time with different relative humidities are illustrated in Fig. 7. From the result of Fig. 7, it can be seen that the water adsorption in shale is very slow, and then gradually diffuses and adsorbs from the exterior to internal until that the moisture humidity inside and outside is equal. Compared with the measured result, we can see that the simulation result of shale particle water vapor is slightly lower than the experimental result, and the reason is that the phase change of water vapor during the simulation is not considered. However, the capillary condensation occurs when the shale particle adsorbs adequate water vapor, which results in the difference between the simulation and the experiment.

6. Conclusions

In this study, the measurements of water adsorption and diffusion from the Longmaxi Fromation shale rocks were carried out at 30 °C and 50 °C for over a relative humidity range of 11.1% to 97.0% using the gravimetric method. Based on the experimental results, a computational model based on the Maxwell-Stefan diffusion equation and the GAB adsorption was constructed to analyze water adsorption and diffusion in shale rocks. According to the above results, the following conclusions can be drawn:

(1) The amount of adsorbed water seems increase linearly at relative pressures below 0.65, while the linear relationship breaks down as the pressure increases and the adsorbed water increases rapidly with pressure. Water adsorption in shale reservoir rocks belongs to the type II isotherm, which includes the monolayer, multilayer adsorption and capillary condensation, and the GAB model can be used to describe the

water adsorption of shale rocks.

(2) Water adsorption by shale is closely related to temperature and the organic carbon content. As the organic carbon content of shale increases, the amount of water adsorption increases, and the organic carbon content and temperature enhance water adsorption in shale at high relative pressures.

(3) The capillary pressure can reach the order of several hundreds of MPa after the hydraulic fracturing process, and the fracturing fluid is far from easy to flow back which results in large amounts of the fracturing fluid remained in shale gas reservoirs. The simulations of water adsorption in shale rocks is below the adsorption experiments, which is an indication that the capillary condensation occurs in shale pores.

Acknowledgments

This work was supported by the National Natural Science Foundation of China (NO. 11802312 and NO. U1762216), and by Open Fund (PLN201810) of State Key Laboratory of Oil and Gas Reservoir Geology and Exploitation (Southwest Petroleum University). We also thank the support from the Youth Foundation of Key Laboratory for Mechanics in Fluid Solid Coupling Systems, Chinese Academy of Sciences.

References

Adamson, A.W., Gast, A.P. Physical Chemistry of Surfaces. New York, John Wiley & Sons, 1967.

Ai-Awad, M.N.J., Smart, B.G.D. Characterization of shale-drilling fluid interaction mechanisms related to wellbore instability. Journal of King Saud University - Engineering Sciences 1996, 8(2): 187-214.

Anderson, R.B. Modifications of the Brunauer, Emmett, and Teller equation. J. Am. Chem. Soc. 1946, 68(4): 686-691.

Boer, J.H. The Dynamic Character of Adsorption. Oxford, Clarendon Press, 1953.

Chang, M., Zhou, J., Chenevert, M.E., et al. The impact of shale preservation on the petrophysical properties of organic-rich shales. Paper SPE166419 Presented at SPE Annual Technical Conference and Exhibition, New Orleans, Louisiana, 30 September - 2 October, 2013.

Chenevert, M.E. Shale control with balanced-activity oil-continuous muds. J. Petrol. Technol. 1970, 22(10): 1309-1316.

Chenevert, M.E., Pernot, V. Control of shale swelling pressures using inhibitive water-base muds. Paper SPE49263 Presented at SPE Annual Technical Conference and Exhibition, New Orleans, Louisiana, 27-30 September, 1998.

Cheng, Y. Impact of water dynamics in fractures on the performance of hydraulically fractured wells in gas shale reservoirs. J. Can. Petrol. Technol. 2012, 51(2): 143-151.

COMSOL. Sweden, COMSOL Inc., 2015.

Dehghanpour, H., Lan, Q., Saeed, Y., et al. Spontaneous imbibition of brine and oil in gas shales: Effect of water adsorption and resulting microfractures. Energ. Fuel. 2013, 27(6): 3039-3049.

Foo, K.Y., Hameed, B.H. Insights into the modeling of adsorption isotherm systems. Chem. Eng. J. 2010, 156(1): 2-10.

Frenkel, J. Kinetic Theory of Liquids. Oxford, Oxford University Press, 1946.

Gao, S., Hu, Z., Guo, W., et al. Water absorption characteristics of gas shale and the fracturing fluid flowback capacity. Nat. Gas Ind. 2013, 33(12): 71-76.

Ge, H., Yang, L., Shen, Y., et al. Experimental investigation of shale imbibition capacity and the factors influencing loss of hydraulic fracturing fluids. Petrol. Sci. 2015, 12(4): 636-650.

Genuchten, M.T.V. A closed-form equation for predicting the hydraulic conductivity of unsaturated soils. Soil Sci. Soc. Am. J. 1980, 44(5): 892-898.

Greenspan, L. Humidity fixed-points of binary saturated aqueous solutions. J. Res. Nat. Bur. Stand. Sect. A 1977, 81(1): 89-96.

Guggenheim, E.A. Application of Statistical Mechanics. Oxford, Clarendon Press, 1966.

Halsey, G.D.J. Physical adsorption on non-uniform surfaces. J. Chem. Phys. 1948, 16(10): 931-937.

Hill, T.L. Advances in catalysis. J. Chem. Phys. 1949, 17: 580-668.

International Energy Agency. World Energy Outlook 2018. Paris, IEA/OECD, 2018.

King, G.E. Thirty years of gas shale fracturing: What have we learned? Paper SPE133456 Presented at SPE Annual Technical Conference and Exhibition, Florence, Italy, 19-22 September, 2010.

Li, J., Li, X., Wu, K., et al. Thickness and stability of water film confined inside nanoslits and nanocapillaries of shale and clay. Int. J. Coal Geol. 2017, 179: 253-268.

Li, Q., Xing, H., Liu, J., et al. A review on hydraulic fracturing of unconventional reservoir. Petrol. 2015, 1(1): 8-15.

Makhanov, K., Habibi, A., Dehghanpour, H., et al. Liquid uptake of gas shales: A workflow to estimate water loss during shut-in periods after fracturing operations. J. Unconv. Oil Gas Res. 2014, 7: 22-32.

Odusina, E.O., Sondergeld, C.H., Rai, C.S. An NMR study of shale wettability. Paper SPE147371 Presented at SPE Canadian Unconventional Resources Conference, Calgary, Alberta, Canada, 15-17 November, 2011.

Prost, R., Benchara, A., Huard, E. State and location of water adsorbed on clay minerals: Consequences of the hydration and swelling-shrinkage phenomena. Clay Clay Miner. 1998, 46 (2): 117-131.

Qi, R., Ning, Z., Wang, Q., et al. Sorption measurements of moistureequilibrated shale with the consideration of water vapor pressure. Sci. Sin. Tech. 2018, 48(5): 524-536.

Shang, S., Horne, R.N., Jr, H.J.R. Water vapor adsorption on geothermal reservoir rocks. Geothermics 1995, 24(4): 523-540.

Shen, W., Li, X., Lu, X., et al. Experimental study and isotherm models of water vapor adsorption in shale rocks.

J. Nat. Gas Sci. Eng. 2018, 52: 484-491.

Shen, W., Li, X., Xu, Y., et al. Gas flow behavior of nanoscale pores in shale gas reservoirs. Energies 2017, 10(6): 1-12.

Shen, W., Xu, Y., Li, X., et al. Numerical simulation of gas and water flow mechanism in hydraulically fractured shale gas reservoirs. J. Nat. Gas Sci. Eng. 2016, 35: 726-735.

Shen, W., Zheng, L., Oldenburg, C.M., et al. Methane diffusion and adsorption in shale rocks: A numerical study using the dusty gas model in Tough2/EOS7C-ECBM. Transport Porous Med. 2018, 123(3): 521-531.

Shen, Y., Ge, H., Su, S., et al. Imbibition characteristic of shale gas formation and water-block removal capability. Sci. Sin-Phys. Mech. Astron. 2017, 47: 114609.

Tandanand, S. Moisture adsorption rate and strength degradation of Illinois shales. Paper ARMA-85-0591-1 Presented at The 26th U.S. Symposium on Rock Mechanics (USRMS), Rapid City, South Dakota, 26-28 June, 1985.

Tien, C. Adsorption Calculations and Modeling. Boston, Butterworth-Heinemann, 1994.

Tokunaga, T.K., Shen, W., Wan. J., et al. Water saturation relations and their diffusion-limited equilibration in gas shale: Implications for gas flow in unconventional reservoirs. Water Resour. Res. 2017, 53(11): 9757-9770.

Wei, M., Duan, Y., Fang, Q., et al. Mechanism model for shale gas transport considering diffusion, adsorption/desorption and Darcy flow. J. Cent. South Univ. 2013, 20(7): 1928-1937.

Wei, M., Duan, Y., Fang, Q., et al. Production decline analysis for a multi-fractured horizontal well considering elliptical reservoir stimulated volumes in shale gas reservoirs. J. Geophys. Eng. 2016, 13(3): 354-365.

Wu, Q., Bai, B., Ma, Y., et al. Optic imaging of two-phase-flow behavior in 1D nanoscale channels. SPE J. 2014, 19(5): 793-802.

Xu, J., Guo, C., Wei, M., et al. Production performance analysis for composite shale gas reservoir considering multiple transport mechanisms. J. Nat. Gas Sci. Eng. 2015, 26: 382-395.